MELTING HEAT TRANSFER OF UNSTEADY MHD BOUNDARY LAYER FLOW OF EYRING-POWELL NANOFLUID PAST AN INCLINED STRETCHING SHEET

VIJAYA BHASKAR REDDY.N*[1], KISHAN NAIKOTI[2]

**[1]Government Degree College (Autonomous),
Siddipet Dist., Telangana state, India, 502103.**

**[2]Department of Mathematics, University College of Science,
Osmania University, Hyderabad, Telangana state, India, 500007.**

ABSTRACT

This paper deals with the viscous incompressible magnetohydrodynamic boundary layer unsteady flow of an Eyring-Powell nanofluid over an inclined melting stretching sheet in the presence of radiation and non-uniform heat source/sink effects has been investigated numerically. The resulting nonlinear governing partial differential equations with associated boundary conditions of the problem has formulated and transformed into a non-similar form. The resultant equations are then solved numerically using Runge-Kutta fourth order method along with shooting technique. The physical significance of different parameters on the velocity, temperature and nanoparticle volume fraction profiles are discussed through graphical illustrations. The impact of physical parameters on local skin friction coefficient, the rate of heat transfer and rate of mass transfer are shown in the tabulated form.

Keywords: Eyring-Powell fluid, Melting heat transfer, MHD, Inclined Stretching sheet, Brownian motion, Radiation, Unsteady.

1. INTRODUCTION

The study of heat transfer over a stretching surface has significant importance due to numerous applications in industrial and technological processes such as cooling of metallic sheets, glass fibres, extrusion of the polymer sheet, and boundary layer along liquid films in concentration processes, paper production and metal spinning. The rate of heat transfer at the stretching surface affects deeply the quality of the final products which must fulfil the desired specifications. Crane [1] was the first investigated an exact analytical solution for the steady two-dimensional flows due to a stretching surface in a quiescent fluid. After this pioneering work, theflow field over a stretching surface has drawn considerable attention and a good amount of research has been investigated on this problem [2–5].

The mathematical formulation forflows of non -Newtonian fluids , in general, is more complex. The most frequently used models of non-Newtonian models are the second grade, Maxwell, Oldroyd-B and power law. A broad description of the behaviour in both steady and unsteadyflow situations, together with mathematical models can be found in Refs . [6–10]. The Powell-Eyring model has certain advantages over the other non-Newtonian fluid models. Firstly, it is deduced from the kinetic theory of liquids rather than the empirical relation. Secondly, it correctly reduces to Newtonian behaviour for low and high shear rates. The study of Powell-Eyring fluid has attracted the researchers of fluid dynamics due to its numerous applications in science and technology. Patel and Timol[11] numerically examined the flow of Powell-Eyring model through asymptotic boundary conditions. Hayat *et al.* [12] studied the steady flow of Powell-Eyring fluid over a moving surface with convective boundary conditions. Flow and heat transfer of Powell-Eyring fluid over shrinking surface in a parallel free stream is presented by Rosca and Pop [13]. Jalil *et al.* [14] studied the flow and heat transfer of Powell-Eyring fluid over a moving surface in a parallel free stream. The problem of slider bearing lubricated with Eyring Powell model is presented numerically using Homotopy perturbation analysis by Islam *et al.* [15]. Regarding the study of Powell-Eyring on fluid flow and heat transfer, some former attentions have been made in the studies [16, 17]. The flow and heat transfer of Powell-Eyring fluid over a continuously moving surface in the presence of a free stream velocity is investigated by Hayat *et al.* [18].

Corresponding Author: Vijaya Bhaskar Reddy.N[1],
[1]Government Degree College (Autonomous), Siddipet Dist., Telangana state, India, 502103.

Due to the small size and very large specific surface areas of nanoparticles, nanofluids have superior properties like high thermal conductivity, minimal clogging in flow passages, long-term stability, and homogeneity. Thus, nanofluids have a wide range of potential applications in electronic cooling, pharmacological administration mechanisms, peristaltic pumps for diabetic treatments, solar collectors and nuclear applications. Based on these real-world applications, Choi[19] has introduced the concept of nanofluid in order to develop advanced heat transfer fluids with substantially higher conductivities. Later on, the boundary layer flow of nanofluid past a stretching surface under the effect of Brownian motion and thermophoresis was investigated by Khan and Pop [20]. Kuznetsov and Nield [21] investigated the natural convective boundary-layer flow of nanofluid past a vertical plate by incorporating Brownian motion and thermophoresis effects. Gorla *et al.* [22] have reported the numerical solutions for a steady boundary layer flow of nanofluid on a stretching circular cylinder in a stagnant free stream. Rajesh Vemula *et al.* [23] analyzed unsteady MHD Free convection flow of nanofluid past an accelerated vertical plate with variable temperature and thermal radiation. The unsteady two-dimensional flow of a non-Newtonian fluid over a stretching surface having a prescribed surface temperature is investigated by Mukhopadhyay *et al.* [24].

Melting and solidification play a vital role in the advanced technology process. Researchers are interested to explore melting heat transfer due to a wide range of application of melting phenomenon of solid-liquid phase change materials in the welding process, crystal growth, thermal protection, heat transportation melting of permafrost, preparation of semiconductors material and the casting of a manufacturing process. Initially, Robert [25] described the melting phenomenon of ice slab placed in a hot air stream. Boundary layer stagnation point flow of Maxwell fluid towards a stretching sheet with melting phenomenon is analyzed by Hayat *et al.* [26]. Das [27] discussed the melting phenomenon in the magnetohydrodynamic flow over a moving surface with thermal radiation. Melting heat transfer in steady laminar flow over a stationary flat plate has been studied by Epstein and Cho [28] Then after, Kazmierczak *et al.* [29] studied the steady convection flow over a flat plate embedded in a porous medium with melting heat transfer effect. Gorla *et al.* [30] have studied the melting heat transfer in mixed convection flow over a vertical plate. Recently, an analysis has been carried out by Bachok *et al.* [31] to analyze a steady two-dimensional stagnation point flow and heat transfer over a melting stretching sheet.

Over the last few years, a considerable amount of experimental and theoretical work has been carried out to determine the role of natural convection in the kinetics of heat transfer accompanied with melting or solidification effect. Processes involving melting heat transfer in non-Newtonian fluids have promising applications in thermal engineering, such as oil extraction, magma, solidification, melting of permafrost, geothermal energy recovery, silicon wafer process, thermal insulation, etc. Chamkha *et al.* [32] analysed the effect of the transverse magnetic field on hydromagnetic, forced convection flow with heat and mass transfer of a nanofluid over a horizontal stretching plate under the influence of melting and heat generation or absorption. Gorla *et al.* [33] presented a boundary layer analysis for a warm and laminar flow of nanofluid over a melting surface moving parallel to a uniform free stream.

Recently, P. Mohan Krishna, N. Sandeep *et al.* [38] investigated the unsteady flow of Powell Eyring fluid past an inclined stretching sheet in the presence of radiation, non-uniform heat source/sink and chemical reaction. The main emphasis of the current paper deals with the two-dimensional unsteady flow of a Powell-Eyring nanofluid past a melting stretching inclined in the presence of radiation and non-uniform heat source/sink with chemical reaction. To achieve this study the suitable transformation is used to transform the partial differential equations to a system of ordinary differential equations together with boundary Conditions the resulting system of ordinary differential equations are solved using the well-known Runge-Kutta technique along with shooting method.

2. MATHEMATICAL FORMULATION

Consider an incompressible, two-dimensional unsteady MHD boundary layer flow of an electrically conducting Powell-Eyring fluid past an inclined stretching sheet in the presence of nanoparticles. A magnetic field of strength $B_0(t)$ is applied normal to the sheet along the y-direction. It is also assumed that, T_m and C_m represents the surface temperature and concentration of nanoparticles at the sheet respectively, while T_∞ and C_∞ respectively denote the ambient fluid temperature and concentration. It is assumed that the Reynolds number is small so that an induced magnetic field is neglected. The applied transverse magnetic field is assumed to be variable kind and is considered in the special form as $B(t) = \frac{B_0}{(1-at)^{1/2}}$. The sheet makes an angle α with the vertical direction and the *x*-axis is taken along the sheet and *y*-axis is normal to it. In addition, we considered the effects of thermal radiation, chemical reaction and non-uniform heat source/sink.

The Cauchy stress tensor in Powell-Eyring fluid is given by

$$\tau_{ij} = \mu \frac{\partial u_i}{\partial x_j} + \frac{1}{\beta} sinh^{-1}\left(\frac{1}{c_1}\frac{\partial u_i}{\partial x_j}\right)$$

In which μ stands for dynamic viscosity β and c_1 for material fluid constants. Considering

$$sinh^{-1}\left(\frac{1}{c_1}\frac{\partial u_i}{\partial x_j}\right) \cong \frac{1}{c_1}\frac{\partial u_i}{\partial x_j} - \frac{1}{6}\left(\frac{1}{c_1}\frac{\partial u_i}{\partial x_j}\right)^3, \left|\frac{1}{c_1}\frac{\partial u_i}{\partial x_j}\right| \ll 1$$

The boundary layer expressions for two-dimensional magnetohydrodynamic flow of Powell-Eyring nanofluid are as follows(see Rosca and Pop[13], Jalil *et al.* [14]):

$$\frac{\partial u}{\partial x} + \frac{\partial v}{\partial y} = 0 \tag{1}$$

$$\frac{\partial u}{\partial t} + u\frac{\partial u}{\partial x} + v\frac{\partial u}{\partial y} = \nu\frac{\partial^2 u}{\partial y^2} + \frac{1}{\rho\beta c_1}\frac{\partial^2 u}{\partial y^2} - \frac{1}{\rho\beta c_1^3}\left(\frac{\partial u}{\partial y}\right)^2\frac{\partial^2 u}{\partial y^2} \frac{\sigma}{\rho}B^2(t)u + [gB_T(T - T_\infty) + gB_c(C - C_\infty)]cos\alpha \tag{2}$$

$$\frac{\partial T}{\partial t} + u\frac{\partial T}{\partial x} + v\frac{\partial T}{\partial y} = \frac{k}{\rho c_p}\frac{\partial^2 T}{\partial y^2} - \frac{1}{\rho c_p}\frac{\partial q_r}{\partial y} + \tau\left[D_B\frac{\partial C}{\partial y}\frac{\partial T}{\partial y} + \frac{D_T}{T_\infty}\left(\frac{\partial T}{\partial y}\right)^2\right] + q''' \tag{3}$$

$$\frac{\partial C}{\partial t} + u\frac{\partial C}{\partial x} + v\frac{\partial C}{\partial y} = \left[D_B\frac{\partial^2 C}{\partial y^2} + \frac{D_T}{T_\infty}\frac{\partial^2 T}{\partial y^2}\right] - k_l(C - C_\infty) \tag{4}$$

Where t is the time, u and v are the velocity components along x- and y-axis, ε and δ are Powell-Eyring fluid parameters, $\nu\left(=\frac{\mu}{\rho_f}\right)$ stands for kinematic viscosity, k is the thermal conductivity of the fluid, ρ_f is the fluid density, T is the fluid temperature, C is the fluid nanoparticle volume fraction, $\tau\left(=\frac{(\rho c)_p}{(\rho c)_f}\right)$ is the ratio between the effective heat capacity of the nanoparticle material and heat capacity of the fluid(see Oyelakin et al. [37]), D_T for thermophoresis diffusion constant, D_B for Brownian diffusivity constant, c_p is the specific heat, g is the acceleration due to gravity, β_T and β_C is the volumetric coefficient of thermal and mass exponential, K_l is the chemical reaction parameter, $q_r = -\frac{16\sigma^*T_\infty^3}{3k^*}\frac{\partial T}{\partial y}$ is the linearized radiative heat flux, α is the inclined angle, is k^* the mean absorption coefficient, σ^* is the Stefan-Boltzmann constant, is the non-uniform heat source/sink per unit volume. The non-uniform heat source/sink, q''' is modelled by the following expression

$$q''' = \frac{kU_m(x,t)}{xv}[A^*(T_m - T_\infty)f' + B^*(T - T_\infty)]$$

In which A^* and B^* are the coefficients of space and temperature dependent heat source/sink, respectively. Here two cases arise, for internal heat generation $A^* > 0$ and $B^* > 0$ and for internal heat absorption, we have $A^* < 0$ and $B^* < 0$.

The surface velocity is denoted by $u_m(x,t) = \frac{bx}{(1-at)}$

where as the surface temperature is $T_m(x,t) = T_\infty + T_{ref}\frac{bx^2}{v}(1 - at)^{-3/2}$ and surface concentration is

$C_m(x,t) = C_\infty + C_{ref}\frac{bx^2}{v}(1 - at)^{-3/2}$ and time dependent magnetic field $B(t)$ is $B(t) = \frac{B_0}{(1-at)^{1/2}}$.

Here b is the initial stretching rate, a is the positive constant which measures the unsteadiness. Also T_{ref}, C_{ref} are constant reference temperature and nanoparticle volume fraction respectively.

The associated boundary conditions are

$$u = u_m(x,t), T = T_m(x,t), C = C_m(x,t) \text{ at } y = 0 \tag{5}$$

$$u \to 0, T \to T_\infty, C \to C_\infty \text{ as } y \to \infty \tag{6}$$

$$\text{And } k\left(\frac{\partial T}{\partial y}\right)_{y=0} = \rho[\lambda + C_s(T_m - T_0)]v(x,0) \tag{7}$$

and $u_m(x,t) = \frac{bx}{(1-at)}$ here b is the initial stretching rate, a is the positive constant which measures the unsteadiness.

We have $\frac{b}{(1-at)}$ in the initial stretching rate that increases with time, T_m, C_m are the surface temperature and surface concentration and T_∞, C_∞ are the ambient fluid temperature and concentration respectively. Further, k is the thermal conductivity, λ is the latent heat of the fluid and c_s is the heat capacity of the solid surface. Equation (7) states that the heat conducted to the melting surface is equal to the heat of melting plus the sensible heat required to raise the solid surface temperature T_0 to its melting temperature T_m.

Introducing the following similarity transformations

$$\left.\begin{array}{l} u = \frac{bx}{(1-at)}f'(\eta), v = -\sqrt{\frac{vb}{(1-at)}}f(\eta) \\ \eta = y\sqrt{\frac{b}{v(1-at)}}, \theta(\eta) = \frac{T-T_\infty}{T_m-T_\infty}, \phi(\eta) = \frac{C-C_\infty}{C_m-C_\infty} \end{array}\right\} \tag{8}$$

By using above similarity transformations the equations (1) -(4)   reduces to

$$(1 + \epsilon)f''' + ff'' - f'^2 - \epsilon\delta f''^2 f''' - A\left(f' + \frac{1}{2}\eta f''\right) - Mf' + [Gr\theta + Gc\phi]\cos\alpha = 0 \tag{9}$$

$$\left(1 + \frac{4}{3}Rd\right)\theta'' + Pr\left(f\theta' - 2f'\theta - \frac{1}{2}A(3\theta + \eta\theta') + Nb\theta'\phi' + Nt\theta'^2\right) + A^*f' + B^*\theta = 0 \tag{10}$$

$$\phi'' - Le\left[2\phi f' - f\phi' + \frac{1}{2}A(3\phi + \eta\phi') + Kr\phi\right] + \frac{Nt}{Nb}\theta'' = 0 \tag{11}$$

and the boundary conditions(5)-(7) are reduced to

$$\left.\begin{array}{l} Prf[0] + Me\theta'[0] = 0, f'[0] = 1, \theta[0] = 1, \\ \phi[0] = 1, f'[\infty] \to 0, \theta[\infty] \to 0, \phi[\infty] \to 0 \end{array}\right\} \tag{12}$$

Here ϵ and δ stand for fluid parameters, Pr for Prandtl number, Me is the dimensionless melting parameter, M for magnetic parameter, Gr for thermal Grashof number, Gc for solutal Grashof number, Nt for thermophoresis parameter, Nb for Brownian motion parameter and Le for Lewis number, Rd for radiation parameter, A for unsteadiness parameter, Kr for chemical reaction parameter.

These parameters are defined by

$$\left.\begin{array}{l} Pr = \frac{\mu c_p}{k}, \epsilon = \frac{1}{\mu\beta c_1}, \delta = \frac{u_m^3}{2vxc_1^2}, Me = \frac{c_p(T_\infty - T_m)}{\lambda + c_s(T_m - T_0)} Nt = \frac{\tau D_T(T_m - T_\infty)}{vT_\infty} A = \frac{a}{b} \\ Rd = \frac{4\sigma^*T_\infty^3}{kk^*}, Nb = \frac{\tau D_B(C_m - C_\infty)}{v}, Le = \frac{v}{D_B}, Gr = \frac{g\beta_T(T_m - T_\infty)x}{u_s^2}, Gc = \frac{g\beta_c C_\infty}{u_s^2}, Kr = \frac{K_0}{b}. \end{array}\right\} \tag{13}$$

With c_p being the specific heat of the fluid at constant pressure. It is worth mentioning that the melting parameter Me is a combination of the Stefan number $c_p(T_\infty - T_m)/\lambda$ and $c_s(T_m - T_0)/\lambda$ for the liquid and solid phases, respectively. Expressions for the local skin friction coefficient c_{fx} local Nusselt number Nu_x and local Sherwood numberSh_x are defined as,

$$C_{fx} = \frac{\tau_w}{\rho U_w^2}, Nu_x = \frac{xq_w}{K_\infty(T_m - T_\infty)}, Sh_x = \frac{xq_m}{D_B(C_m - C_\infty)}, \tag{14}$$

where k_∞ is the thermal conductivity of the nanofluid, in which wall shear stress τ_w, q_w and q_m are the heat and mass flux, respectively given by

$$\left.\begin{array}{l} \tau_w = \left(\left(1 + \frac{1}{\mu\beta c_1}\right)\frac{\partial u}{\partial y} - \frac{1}{6\mu\beta c_1^3}\left(\frac{\partial u}{\partial y}\right)^3\right)_{y=0} \\ q_w = -K_\infty\left(\frac{\partial T}{\partial y}\right)_{y=0} + (q_r)_w \\ q_m = -D_B\left(\frac{\partial C}{\partial y}\right)_{y=0} \end{array}\right\} \tag{15}$$

Applying similarity transformations (8) for skin friction coefficient and Nusselt number and Sherwood number are converted to

$$\left.\begin{array}{l} Re_x^{\frac{1}{2}}C_{fx} = \left((1 + \epsilon)f''[0] - \left(\frac{\epsilon\delta}{3}\right)f''[0]^3\right), \\ Re_x^{-1/2}Nu_x = -\left(1 + \frac{4}{3}R\right)\theta'[0], Re_x^{-1/2}Sh_x = -\phi[0] \end{array}\right\} \tag{16}$$

Where $Re_x = \frac{U_m(x)x}{v}$ is local Reynolds number.

3. NUMERICAL RESULTS AND DISCUSSION

This section deals with the theoretical and graphical behaviour of different physical quantities which are involving in the present flow problem. The set of coupled non- linear boundary layer equations (9) – (11) together with the boundary conditions (12) does not possess a closed form analytical solution. Hence, it has been solved numerically, using the Runge-Kutta method with a systematic guessing of $f''(0), \theta'(0)$ and $\phi'(0)$ by the shooting technique until the boundary conditions at infinity $f''(\infty), \theta'(\infty)$, and $\phi'(\infty)$ decay exponentially to zero. The value of η_∞ is found to each iteration loop by the assignment statement $\eta_\infty = \eta_\infty + \Delta\eta$. For the purpose of discussing to provide physical insight into the present problem, comprehensive numerical computations are carrying out for various values of the flow parameters which describe the flow characteristics and the results are illustrated graphically. For computational purposes, the reason of integration η is consider as 0 to η_∞ is equivalent to 10, where η_∞ corresponds to $\eta \to \infty$ which lies very well outside the momentum and thermal boundary layer. The step size $\Delta\eta = 0.05$ is used while obtaining the numerical solution and by considering the six decimal place as the criterion for convergence.

The present results are compared with that of Grubka [34], Chen [35] & Sharma [36] and found that were in good agreement between those and present.

A representative set of graphical results for the velocity, temperature and nanoparticle volume fraction as well as skin friction, local nusselt number and local Sherwood number is present and discuss for different flow parameter values. To verify the accuracy of the results we compared our results with those represented by Grubka [34], Chen [35] & Sharma [36] as shown in table1. The results are in excellent agreement between present and the previous results.

Figure1(a)-1(c) explains the effect of melting parameter *Me* on velocity, temperature and nanoparticle volume fraction profiles. It is observed that for increasing value of *Me* the velocity and boundary layer thickness decreases. The temperature distribution decreases with an increasing melting parameter *Me*. This is because an increasing *Me* with increasing the intensity of melting, which acts as blowing boundary conditions at the stretching surface and hence tends to thickness the boundary layer. The effect of melting parameters is to reduces the nanoparticle volume fraction profile.

Figures 2 (a)-2(b) depicts the profiles for velocity and temperature for various values of Radiation parameter *Rd*. It is evident in the figures that an increases Radiation parameter *Rd* is to enhance velocity and temperature profiles This is due to an increasing the Radiation parameter *Rd* releases the more heat energy to the flow field. This causes to enhance velocity and thermal boundary layer. In view of this, it concludes that influence of radiation is more significant as $Rd \to 0 (Rd \neq 0)$ and it can be neglect as $Rd \to \infty$. This agrees the general physical behaviour of the radiation parameter.

The influence of inclined angle on the velocity profile is illustrated in figure (3). It is the fact that as $\alpha = 0$ the sheet is in vertical direction and hence maximum gravitational force acts on the flow and when $\alpha = \pi/2$ the sheet is in horizontal direction, the strength of buoyancy forces decreases and hence reduces the velocity boundary layer.

Figure4 (a)-4(c) illustrates the effect of Prandtl number *Pr* on velocity, temperature and nanoparticle volume fraction. It is seen that the magnitude of the velocity gradient at the surface is higher for higher values of *Pr*. Thus the velocity field increases with an increase the value of *Pr*. It is observed that as increasing *Pr* is leading to decrease the temperature profiles as well as decreases the thermal boundary layer thickness. The nanoparticle volume fraction increases with the increasing Prandtl number value. This is due to the fact that for small values of *Pr* are equivalent to larger values of thermal conductivities and therefore it is able to diffuse away from the stretching sheet.

Figure 5(a)-5(c) elucidates that when Eyring-Powell parameter(ε) increases there is an increase in the velocity profile. Since Eyring-Powell parameter is $\varepsilon = \frac{1}{\rho \beta c_1 \nu}$ and $= \frac{\mu}{\rho}$. So by increasing Eyring-Powell parameter (ε) viscosity of fluid i.e, μ decreases which causes increasing velocity also fluid becomes less viscous for larger values of Eyring-Powell parameter which enhances fluid velocity. It is noticed that the temperature and nanoparticle volume fraction profiles are decreases with an increasing Eyring-Powell parameter.

Figure 6(a)-6(c) is drawn for the effect of unsteadiness parameter *A* on velocity temperature and nanoparticle volume fraction profiles. It is clear from the figure that an increasing unsteadiness parameter *A* reduces the velocity, temperature and nanoparticle volume fraction profiles. At the same time, there is a reduce in the momentum, thermal, concentration boundary layer thickness due to the increasing unsteadiness parameter.

Figure 7 and 8 illustrate the effects of non-uniform heat source/ sink parameters on velocity and temperature profiles. The positive values of A^*, B^* heat is generating and releases the heat energy to the flow. Due to this there is an increase in the velocity, temperature profiles with the increase of A^*, B^* values.

Figure 9(a)-9(c) shows derivations in velocity, temperature and nanoparticle volume fraction profiles for different values of magnetic field parameter *M*. When magnetic field strength increases Lorentz force becomes stronger, which creates resistance in the motion of the fluid, so that velocity profile decreases. It is noticed that the temperature and nanoparticle volume fraction profiles are increases with an increasing magnetic field parameter *M*.

Figure 10(a)-10(c) reflects the effect of Thermophoresis parameter *Nt* on velocity, temperature and nanoparticle volume fraction profiles, respectively. Thermophoresis mechanism in which small particles are pulled away from the hot surface to the cold surface due to this the transportation temperature of the fluid arises. Therefore the effect of thermophoresis parameter *Nt* is to enhance the velocity and temperature profiles. It can be observed that an enhancement in the thermophoresis parameter *Nt* produces a force which leads to the moment of nano particles from a hot region to cold region and hence the nanoparticle volume fraction increases with an increase the value of thermophoresis parameter *Nt*. Figure 11(a)-11(b) shows that the effect of Brownian motion parameter *Nb* on Temperature and nanoparticle volume fraction profiles. The effect of Brownian motion parameter *Nb* is to enhance the temperature profile. It can be observed that the nanoparticle volume fraction decreases by increasing the Brownian motion parameter *Nb*. This holds practically because with an increase in *Nb* the random motion collusion of the macroscopic particles of the fluid increases. This reduces the concentration of the fluid also Brownian motion parameter *Nb* decreases the concentration boundary layer thickness.

Figure (12) display the influence of Lewis number Le on nanoparticle volume fraction profile. It is observed from the figure that an increase in the values of Lewis number depreciates the nanoparticle volume fraction and concentration boundary layer thickness decreases. This is due to the fact that mass transfer rate increases.

Figures (13) and (14) depict the variation of thermal Grashof number (Gr) and solutal Grashof number (Gc) on velocity profile. From figures, it is noticed that an increase in the momentum boundary layer thickness and increasing velocity profiles accompanies with an increasing Gr and Gc. The thermal Grashof number Gr signifies the relative effect of the thermal buoyancy force to the viscous hydrodynamic force in the boundary layer as expecting it is noticed that there is a rise in the velocity profile due to the enhancement of thermal buoyancy force. The solutal Grashof number Gc defines the ratio of the species buoyancy force to the viscous hydrodynamic force due to increasing the species buoyancy force there is an increasing the velocity.

Figure(15) shows that the effect of chemical reaction parameter *(kr)* is to reduces the nanoparticle volume fraction profiles. This is due to the fact that the increasing chemical reaction parameter reduces the concentration boundary layer thickness.

Table-1: Comparison with previously published data for the values of $-\theta'(0)$
when $A^* = B^* = Me = M = \varepsilon = \delta = \alpha = Gr = Gc = A = Rd = Kr = 0$ and without nanoparticles.

Pr	Grubka[34]	Chen[35]	Sharma[36]	Present results
0.72	1.0885	1.08853	1.0885	1.08999
1.00	1.3333	1.33334	1.3332	1.33324
3.00	2.5097	2.50972	2.5092	2.50923
10.0	4.7969	4.79686	4.7945	4.79579

1(a).Velocity

1(b).Temperature

1(c).Nanoparticle volume fraction
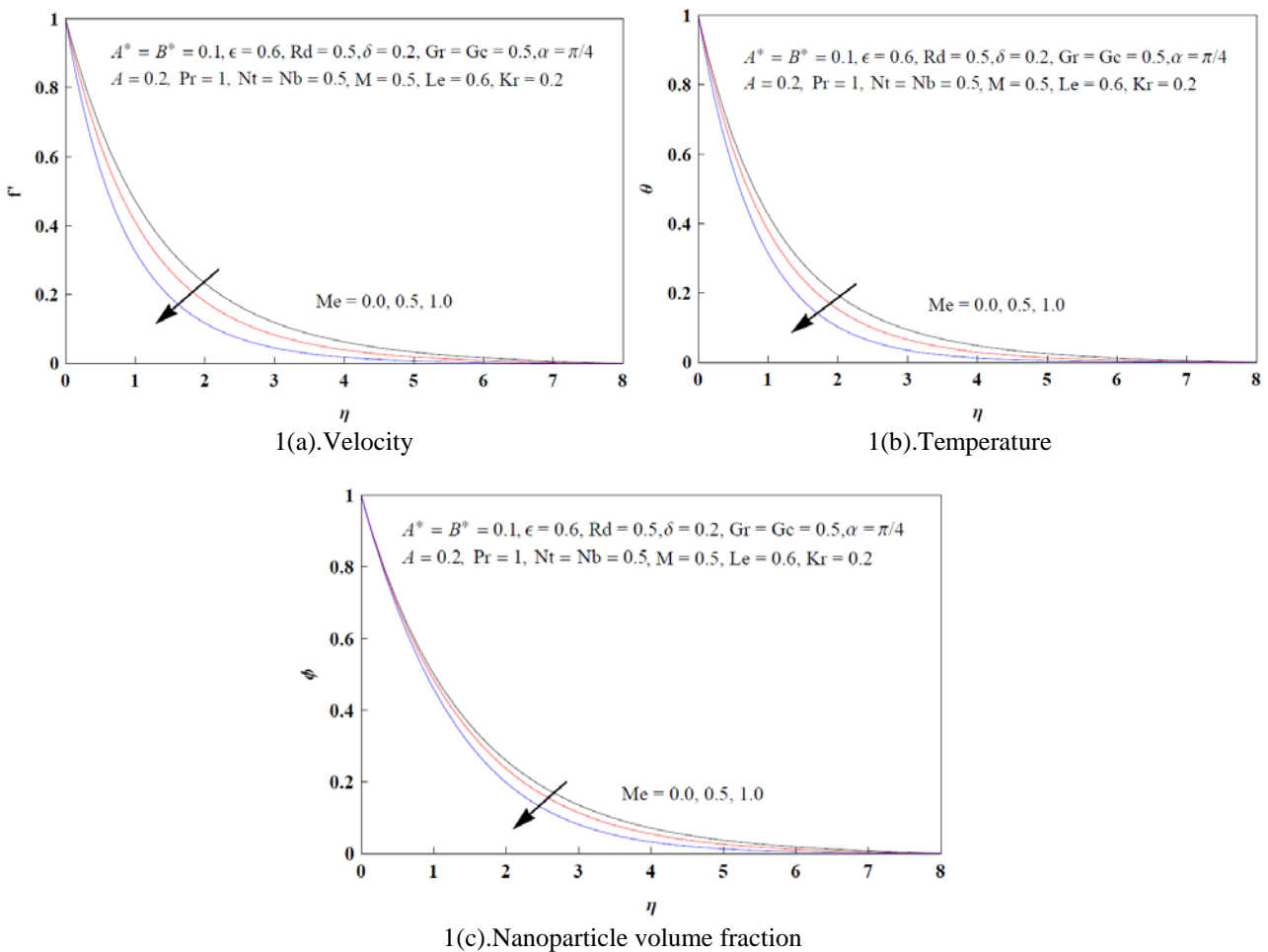
Figure-1: Variation of melting parameter *(Me)* on velocity, temperature and nanoparticle volume fraction profiles
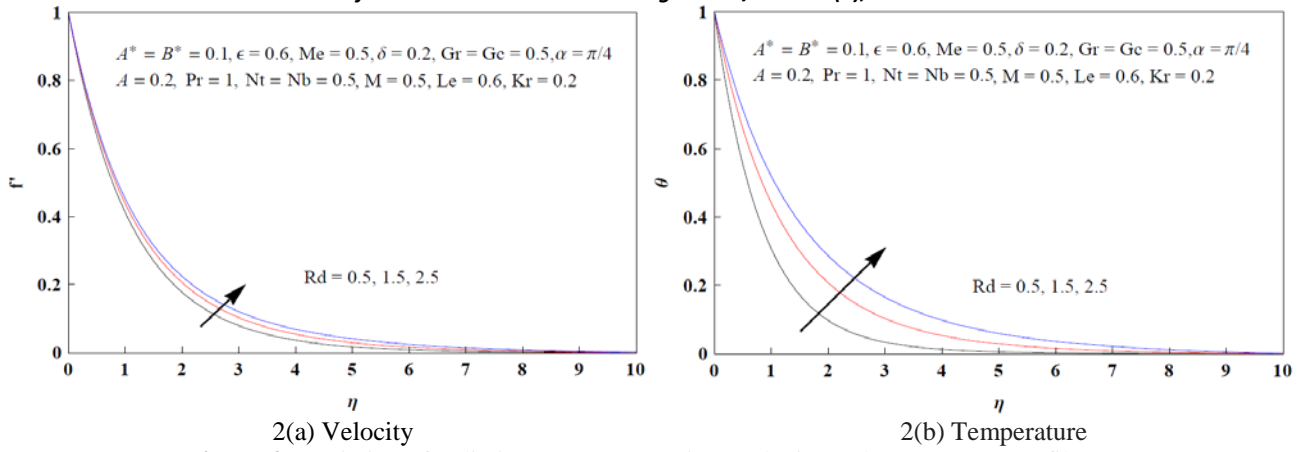
2(a) Velocity

2(b) Temperature

Figure-2: Variation of radiation parameter (*Rd*) on velocity and temperature profiles
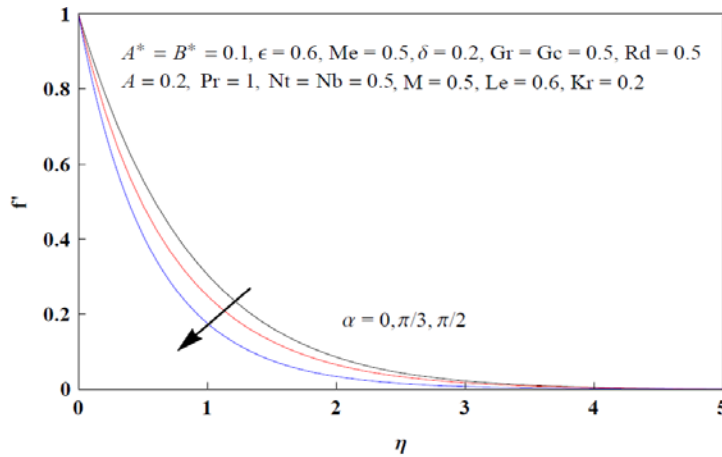

Figure-3: Variation of inclined angle (α) on velocity profile.
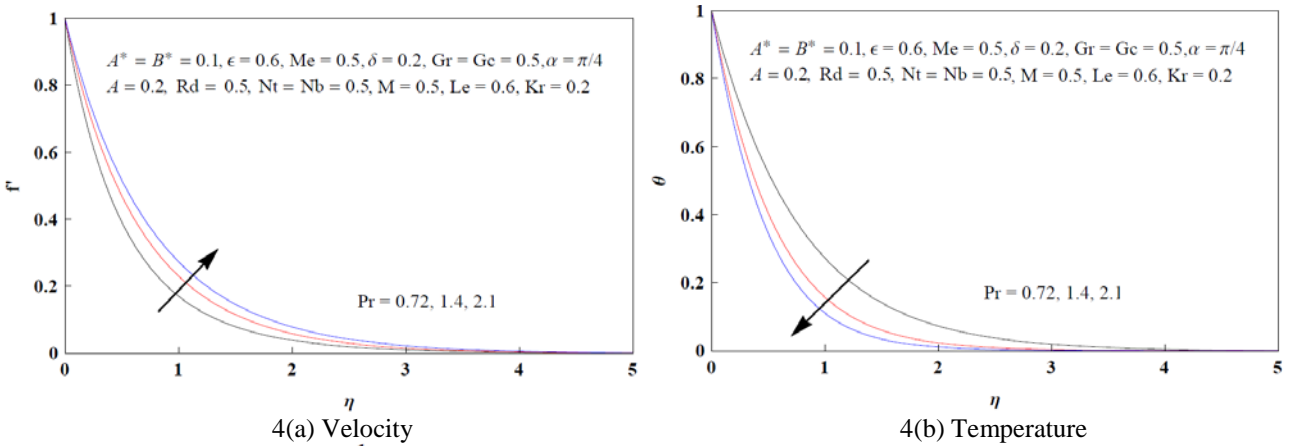
4(a) Velocity

4(b) Temperature

4(c) Nanoparticle volume fraction

Figure-4: Variation of Prandtl number (*Pr*) on velocity, temperature and nanoparticle volume fraction profiles

5(a).Velocity

5(b) Temperature

5(c) Nanoparticle volume fraction
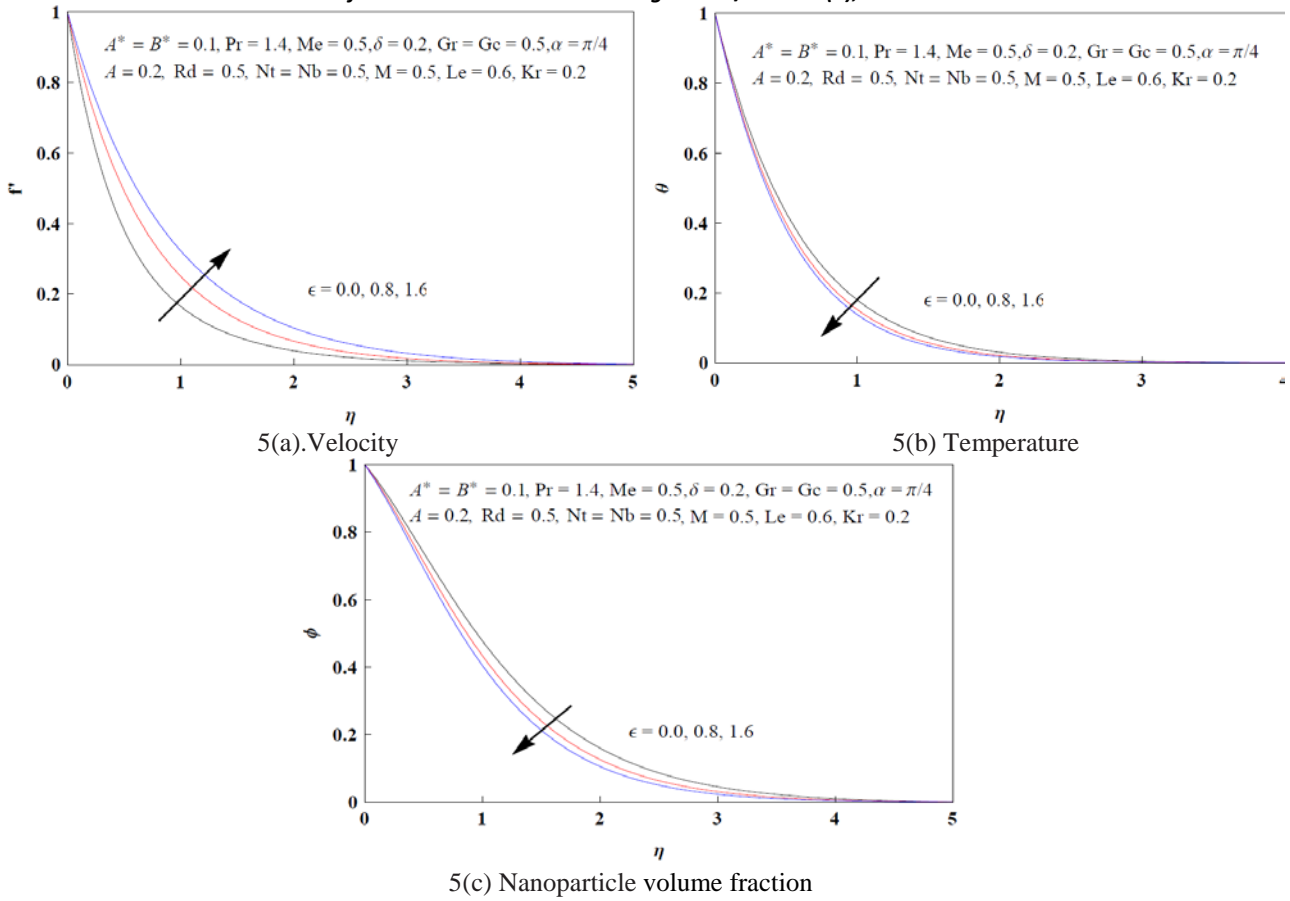
Figure-5: Variation of Eyring-Powell fluid parameter (ε)on velocity, temperature and nanoparticle volume fraction profiles.


6(a) Velocity

6(b) Temperature

6(c) Nanoparticle volume fraction
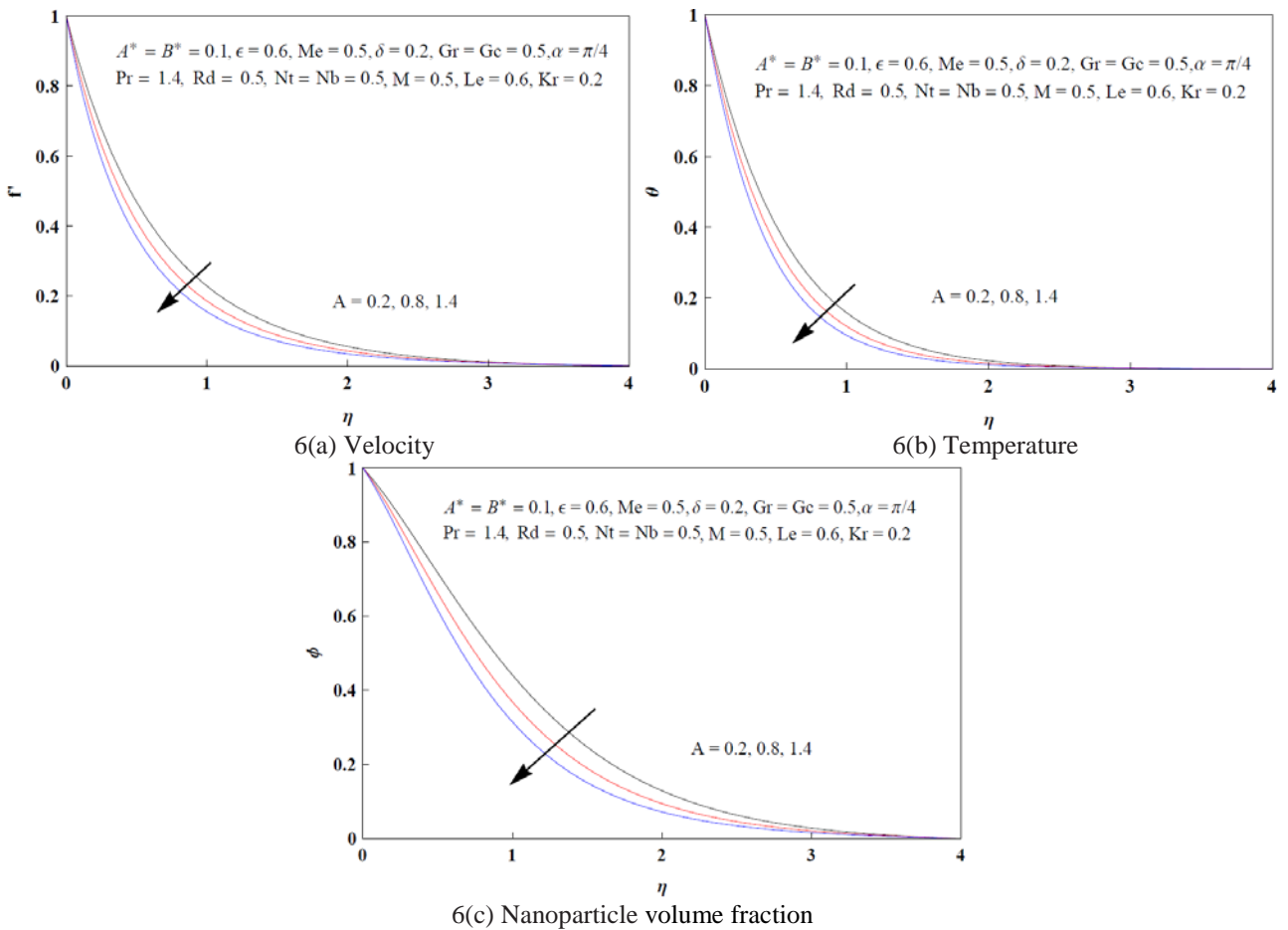
Figure-6: Variation of unsteadiness parameter A on velocity, temperature and nanoparticle volume fraction profiles

7(a) Velocity
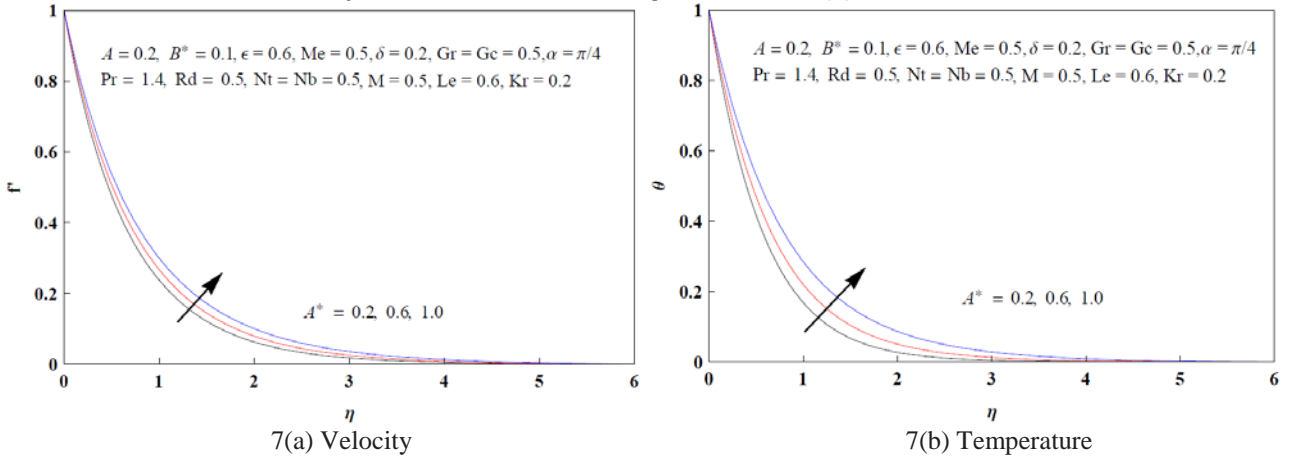
7(b) Temperature

Figure-7: Variation of non-uniform heat source/sink parameter A^* on velocity, temperature profiles

8(a) Velocity
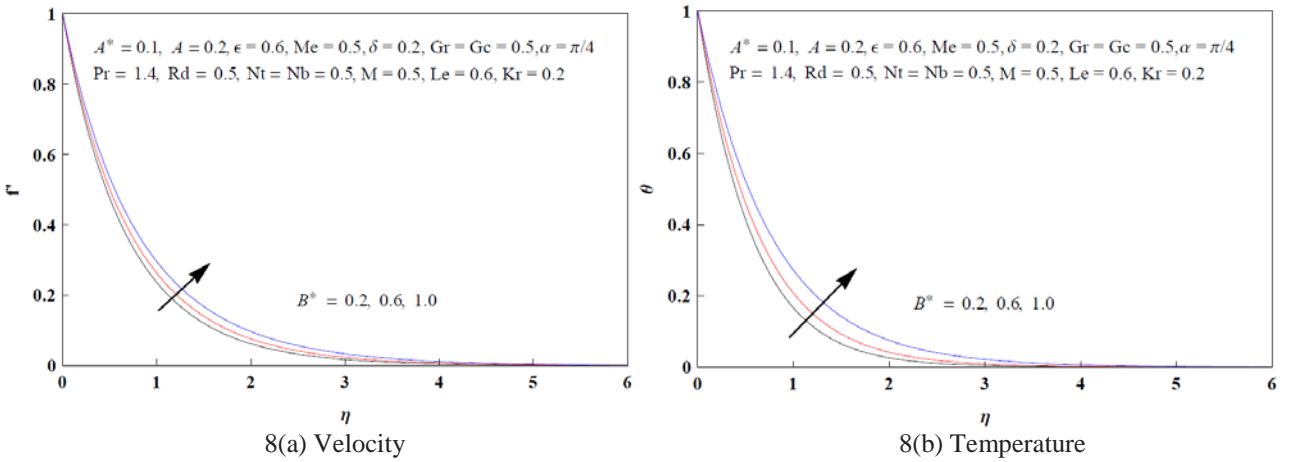
8(b) Temperature

Figure-8: Variation of non-uniform heat source/sink parameter B^* on velocity, temperature profiles

9(a) Velocity

9(b) Temperature

9(c) Nanoparticle volume fraction
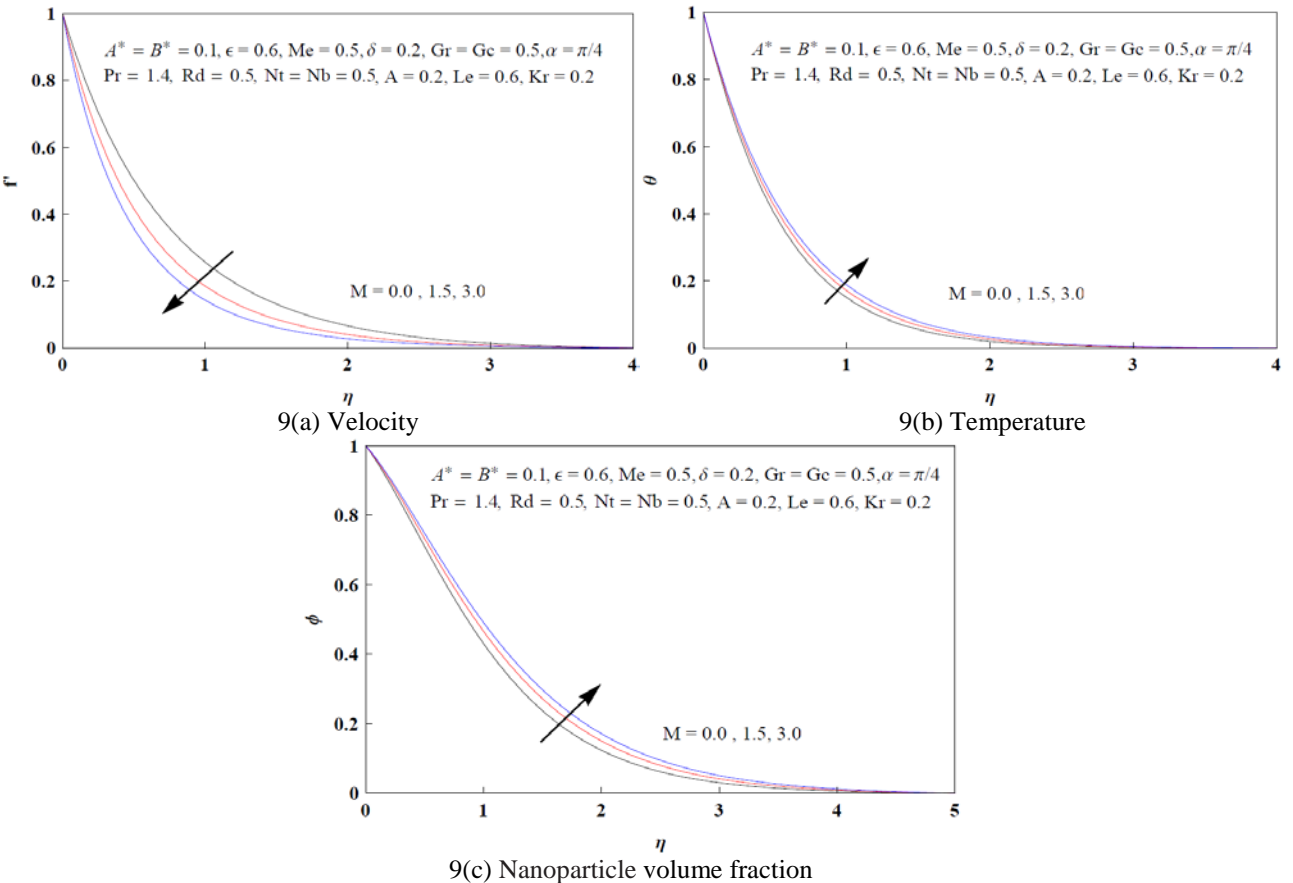
Figure-9: Variation of magnetic field parameter (*M*) on velocity, temperature and nanoparticle volume fraction profiles

10(a) Velocity

10(b) Temperature

10(c) Nanoparticle volume fraction
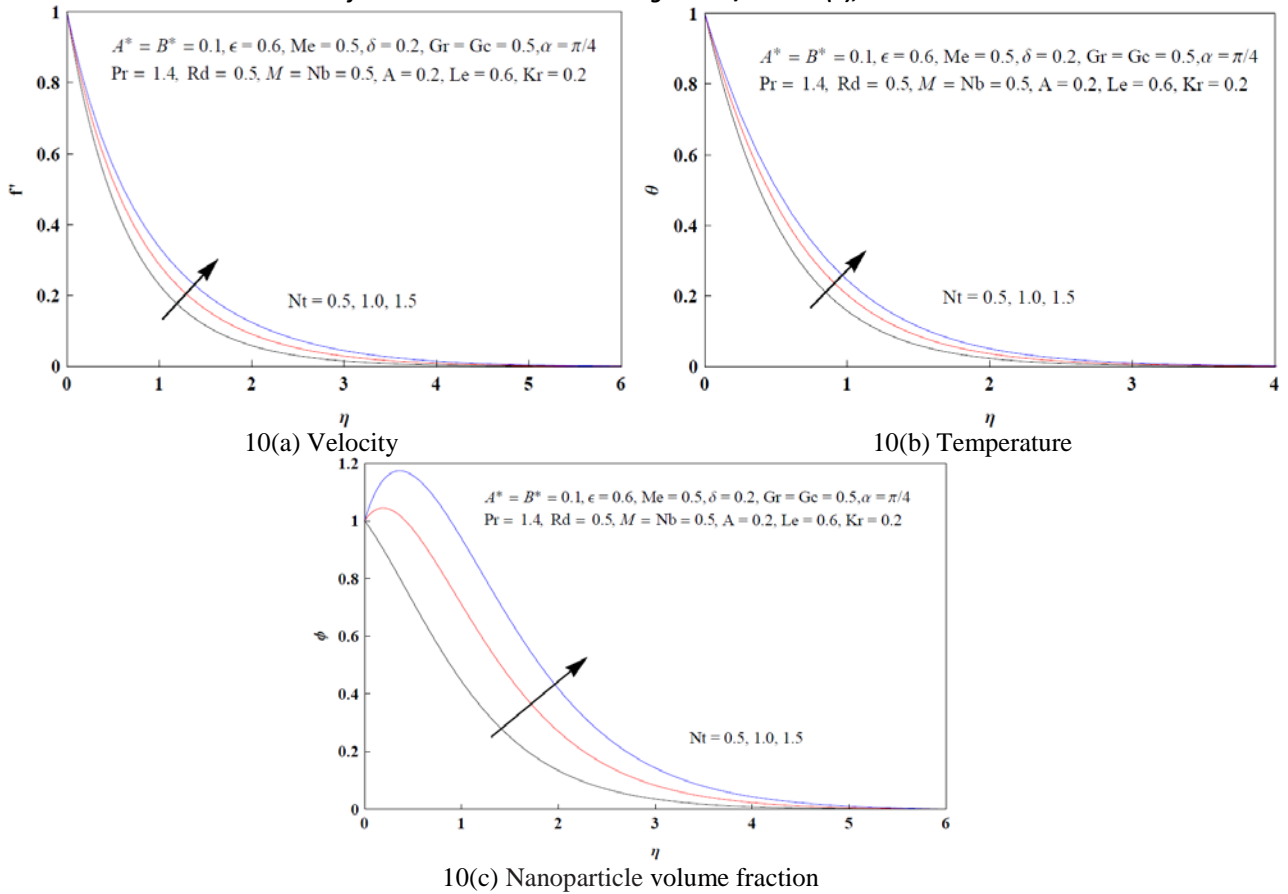
Figure-10: Variation of Thermophoresis parameter *(Nt)* on velocity, temperature and nanoparticle volume fraction profiles



11(a) Temperature


11(b) Nanoparticle volume fraction
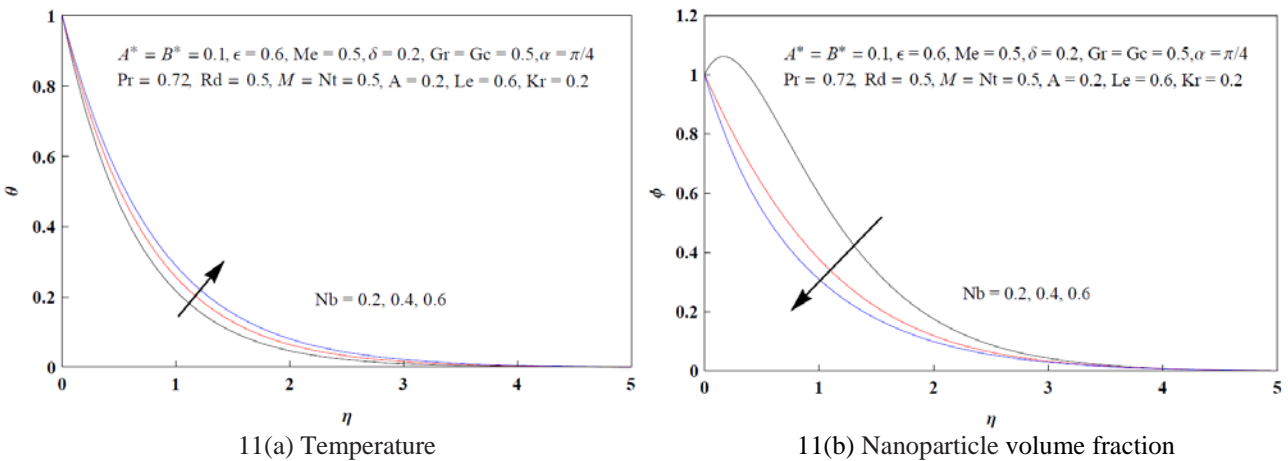
**Figure-11:** Variation of Brownian motion parameter (*Nb*) on temperature and nanoparticle volume fraction profiles
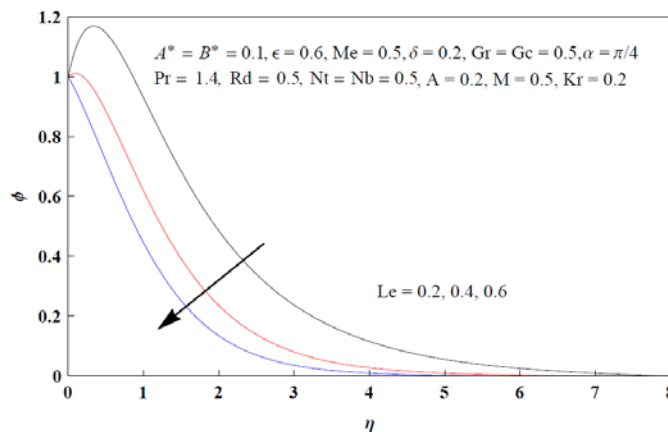
Figure-12: Variation of Lewis number (*Le*) on nanoparticle volume fraction profile
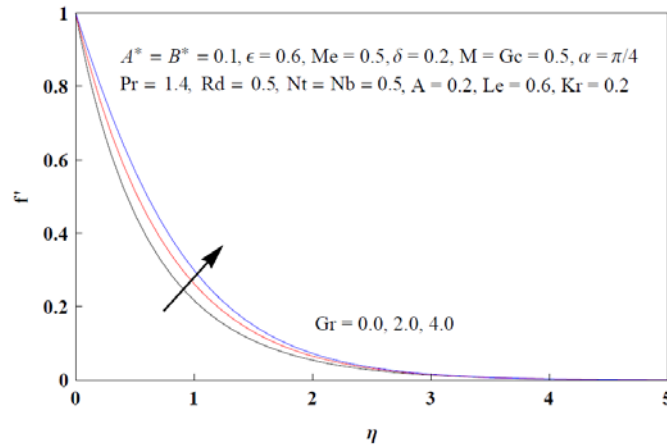
Figure-13: Variation of thermal Grashof number *(Gr)* on velocity profile
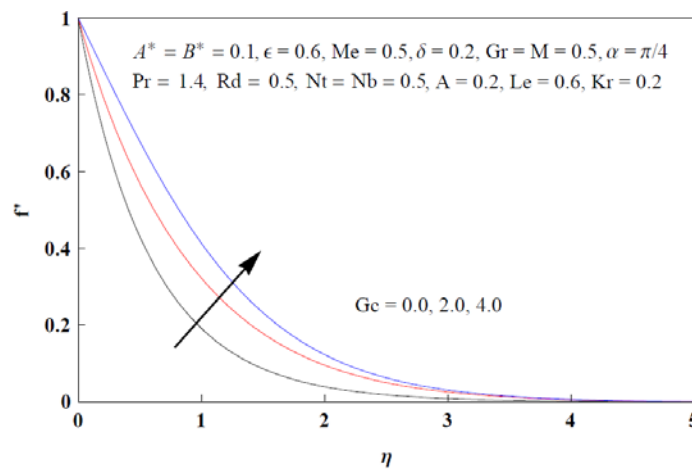
Figure-14: Variation of solutal Grashof number *(Gc)* on velocity profile
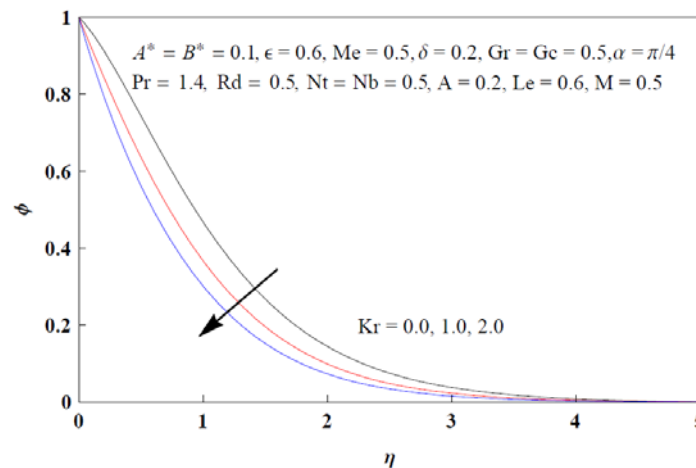
Figure-15: Variation of chemical reaction parameter (Kr) on nanoparticle volume fraction profile

The variation of the dimensionless quantities such as the local skin friction coefficient, local nusslet number and local Sherwood number, for different values of physical parameters $Me, Rd, \varepsilon, M, A, Kr, A^*, B^*, \alpha, Nt, Nb, Le$ are shown in table 2. It can be noticed that skin friction value decreases with the increase of $Me, M. A, Kr, \alpha, Le$ where as it increases with an increasing the values of $Rd, \varepsilon, A^*, B^*, Nt, Nb$. The local Nusselt number decreases with an increasing the values of $Rd, M, Kr, A^*, B^*, \alpha, Nt, Nb, Le$ while it is increasing with Me, ε and A. Finally the local Sherwood number decreases with an increasing the values of M, α, Nt while it is increasing with $Me, Rd, \varepsilon, A, Kr, A^*, B^*, Nb, Le$.

Table-2: Numerical values of local skin friction coefficient, local Nusselt number and local Sherwood number for different values of $Me, Rd, \varepsilon, M, A, Kr, A^*, B^*, \alpha, Nt, Nb, Le$.

Me	Rd	ε	M	A	Kr	A^*	B^*	α	Nt	Nb	Le	c_{fx}	$-Nu_x$	$-\phi'(0)$
0.2	1	1	0.2	0.1	0.1	0.1	0.1	0	0.1	0.1	1	−1.937396	1.933218	1.183869
0.4												−2.054798	2.011725	1.239998
0.6												−2.190510	2.102569	1.303912
0.2	1											−1.937396	1.933218	1.183869
	2											−1.900713	1.458962	1.293382
	3											−1.880101	1.204881	1.347324
	1	0.5										−2.218892	1.872103	1.159093
		1										−1.937396	1.933218	1.183869
		1.5										−1.740928	1.977189	1.201949
		1	0.2									−1.553137	1.933218	1.183869
			0.4									−1.673683	1.899387	1.170197
			0.6									−1.786323	1.867819	1.157600
			0.2	0.1								−1.553137	1.933218	1.183869
				0.3								−1.654172	2.092968	1.246113
				0.5								−1.744609	2.242631	1.281921
				0.1	0.1							−1.553137	1.933218	1.183869
					0.3							−1.555781	1.930340	1.275106
					0.5							−1.557925	1.927988	1.358792
					0.1	0.2						−1.548210	1.855707	1.201416
						0.4						−1.538307	1.699798	1.236342
						0.6						−1.528338	1.542711	1.271031
						0.1	0.2					−1.547593	1.849868	1.201992
							0.4					−1.533696	1.653739	1.241226
							0.6					−1.511522	1.374432	1.287723
							0.1	0				−1.553137	1.933218	1.183869
								$\pi/4$				−1.588180	1.923446	1.179906
								$\pi/3$				−1.611799	1.916666	1.177178
								0	0.1			−1.553137	1.933218	1.183869
									0.2			−1.540106	1.917965	0.805071
									0.3			−1.527417	1.902698	0.438266
									0.1	0.2		−1.557043	1.889365	1.384168
										0.4		−1.555871	1.808970	1.481464
										0.6		−1.552841	1.733262	1.511536
										0.1	1	−1.553137	1.933218	1.183869
											2	−1.568682	1.915761	2.041460
											3	−1.575631	1.907619	2.703694

4. CONCLUSIONS

This present investigation is a worthwhile attempt to study the problem which involves MHD boundary layer unsteady flow and heat transfer for non-Newtonian Powell-Eyring nanofluid flow past an inclined stretching sheet. The computed results were presented graphically and analyzed the effects of the emerging flow parameters on velocity, temperature and nanoparticle volume fraction profiles and discussed in detail with physical interpretations.

- It is found that effects of the flow parameters *M, Me,α, A* is to reduces the non-dimensional velocity profile whereas the velocity profile increases with an increase of *Rd, ε*.
- The effect of A^*, B^* is to enhances the both velocity and temperature profiles, it is noticed that as A, ε increases the temperature and nanoparticle volume fraction profiles decreases as the effect of *Pr* then reduces the temperature profiles and enhances the velocity and nanoparticle volume fraction profiles.
- The effect of Magnetic field parameter *M* is to enhance the temperature and nanoparticle volume fraction profiles, as the effect of Thermophoresis parameter *Nt* is to enhances the velocity, temperature and nanoparticle volume fraction profiles, Whereas the nanoparticle volume fraction profiles decrease with the increases of *Nb* and *Le*.
- Finally, it is found that the skin friction coefficient value increases with the increase of the values $Rd, \varepsilon, A^*, B^*, Nt, Nb$ while it decreases with Me, M, A, Kr, α, Le.

- It is seen that the local Nusslet number value increases with an increasing the values of Me, ε, A while decreases with increasing $Rd, M, Kr, A^*, B^*, \alpha, Nt, Nb, Le$.
- It is also seen that mass transfer coefficient value $-\phi'(0)$ increases with an increasing the values of $Me, Rd, \varepsilon, A, Kr, A^*, B^*, Nb, Le$.while decreases with increasing of M, α, Nt.

5. NOMENCLATURE

x	distance along the surface	$B(t)$	time-dependent magnetic field
y	distance normal to the surface	B_0	intensity of magnetic field
u	velocity component in $x-$direction	ρ	density of fluid
v	velocity component in $y-$direction	ν	kinematic viscosity
t	time	α_m	effective thermal diffusivity
V	velocity field	u_m	stretching velocity
T	temperature field	T_m	surface temperature
C	Nanoparticle volume fraction	C_m	surface nanoparticle concentration
τ_{ij}	extra stress tensor	T_∞	ambient fluid temperature
p	pressure	C_∞	ambient fluid concentration
ε, δ	fluid parameters	D_T	thermophoresis diffusion coefficient
η	local similarity variable	D_B	Brownian diffusion coefficient
f'	dimensionless velocity	k	thermal conductivity
θ	dimensionless temperature	c_p	specific heat capacity
ϕ	imensionless Nanoparticle volume fraction	T_{ref}	reference temperature
β, c_1	material fluid constants	C_{ref}	reference concentration
M	magnetic parameter	a	positive constant
Pr	Prandtl number	b	initial stretching rate
Rd	Radiation parameter	Me	melting parameter
C_{fx}	local skin friction coefficient	Nt	thermophoresis parameter
Nu_x	local Nusselt number	Nb	Brownian motion parameter
Sh_x	local Sherwood number	Le	Lewis number
q_r	linearized radiative heat flux	A	unsteadiness parameter
k^*	mean absorption parameter	τ_w	wall shear stress
σ^*	Stefan-Boltzmann constant	q_w	wall heat flux
q'''	non uniform heat source/sink	q_m	wall mass flux
A^*, B^*	coefficients of space and temperature	θ_w	temperature difference parameter
Gr	thermal Grashof number	Nr	nonlinear thermal radiation parameter
Gc	solutal Grashof number	Kr	chemical reaction parameter
Re	local Reynolds number		

ACKNOWLEDGEMENTS

REFERENCES

1. Crane LJ., *Flow past a stretching plate*, Z Angrew Math Phys (1970), vol.21, pp.645–647.
2. H.I. Andersson, B.S. Dandapat, *Magneto hydrodynamic Flow of a power-law fluid over a stretching sheet*, International Journal of Non-Linear Mechanics(1992), vol.27(6), pp.929-936.
3. E. Magyari, B. Keller, *Exact solutions for self-similar boundary-layer flows induced by permeable stretching walls*, Eur. J. Mech. B Fluids (2000) ,vol.19, pp.109–122.
4. Hunegnaw Dessie, Naikoti Kishan, *MHD effects on heat transfer over stretching sheet embedded in porous medium with variable viscosity, viscous dissipation and heat source/sink*, Ain shams engineering journal(2014),vol.26,pp.967–977.
5. N. Kishan And P. Amrutha, *Effects of viscous dissipation on MHD flow with heat and mass transfer over a stretching surface with heat source, thermal stratification and chemical reaction*, Journal of Naval Architecture and Marine Engineering (2011), vol.7(1), pp.11–18.
6. O.D. Makinde, T. Chinyoka, L. Rundora, *Unsteady flow of a reactive variable viscosity non-Newtonian fluid through a porous saturated medium with asymmetric convective boundary conditions*, Comput. Math. Appl.(2011), vol.62, pp.3343– 3352.

7. Macha Madhu, Naikoti Kishan,*Magneto hydrodynamic mixed convection stagnation-point flow of a power-law non-Newtonian nanofluid towards a stretching surface with radiation and heat source/sink*, Journal of Fluids(2015),vol.2015,pp.1–14.

8. M Madhu, N Kishan, *Finite element analysis of heat and mass transfer by MHD mixed convection stagnation-point flow of a non-Newtonian power-law nanofluid towards a stretching surface with radiation,* Journal of the Egyptian Mathematical Society(2016), vol.24(3), pp.458–470.

9. M Madhu, N Kishan, A Chamka, *Boundary layer flow and heat transfer of a non-Newtonian nanofluid over a non-linearly stretching sheet*, International Journal of Numerical Methods for Heat & Fluid Flow(2016),vol.26(7),pp.2198–2217.

10. M Madhu, N Kishan, *MHD boundary-layer flow of a non-Newtonian nanofluid past a stretching sheet with a heat source/sink*, Journal of Applied Mechanics and Technical Physics(2016),vol.57 (5), pp.908–915.

11. M. Patel, M.G. Timol*, Numerical treatment of Powell-Eyring fluid flow using method of satisfaction of asymptotic boundary conditions*, Appl. Numer. Math.(2009),vol.59 pp.2584– 2592.

12. T. Hayat, Z. Iqbal, M. Qasim, S. Obidat, *Steady flow of an Eyring Powell fluid over a moving surface with convective boundary conditions,* Int. J. Heat Mass Transf.(2012), vol.55 pp.1817– 1822.

13. A.V. Rosca, I.M. Pop, *Flow and heat transfer of Powell-Eyring fluid over a shrinking surface in a parallel free stream,* Int. J. Heat Mass Transf.(2014), vol.71,pp.321–327.

14. M. Jalil, S. Asghar, S.M. Imran, *Self similar solutions for the flow and heat transfer of Powell -Eyring fluid over a moving surface in a parallel free stream,* Int. J. Heat Mass Transf. (2013), vol.65,pp.73–79.

15. S. Islam, A. Shah, C.Y. Zhou, I. Ali, *Homotopy perturbation analysis of slider bearing with Powell-Eyring fluid,* Z. Angew. Math. Phys (2009),vol. 60,pp.1178–1193.

16. V. Sirohi, M.G. Timol, N.L. Kalathia, *Numerical treatment of Powell-Eyring fluid flow past a 90 degree wedge,* Reg. J. Energy Heat Mass Tran(1984) ,vol.6(3), pp.219–228.

17. R.E. Powell, H. Eyring, *Mechanism for relaxation theory of viscosity*, Nature(1944) vol.154,pp.427–428.

18. T. Hayat, Z. Iqbal, M. Qasim, S. Obaidat, *Steady flow of an Eyring-Powell fluid over a moving surface with convective boundary conditions,* Int. J. Heat Mass Transf.(2012) vol.55, pp.1817–1822.

19. S.U.S. Choi, J.A. Eastman, *Enhancing thermal conductivity of fluids with nanoparticles,* ASME Pub. Fed. (1995), Vol.231, pp.99–106.

20. W.A.Khan, I.Pop, *Boundary-layer flow of a nanofluid past a stretching sheet*, Int. J. Heat Mass Transf.(2010), vol.53, Pp .2477-2483.

21. Kuznetsov VA and Nield D A, *Natural convective boundary-layer flow of a nanofluid past a vertical plate,* International Journal of Thermal Sciences, (2010), vol.49(2), pp.243–247.

22. Rama Subba Reddy Gorla ,*Transient response behavior of an axisymmetric stagnation flow on a circular cylinder due to time dependent free stream velocity,* International Journal of Engineering Science(1978), vol.16(7), Pp.493-502.

23. Rajesh Vemula, Lokenath Debnath, Sridevi Chakrala*, Unsteady mhd Free convection flow of nanofluid past an accelerated vertical plate with variable temperature and thermal radiation,* International Journal of Applied and Computational Mathematics(2017), vol.3(2), pp.1271–1287

24. Swati Mukhopadhyay, Prativa Ranjan.De, Krishnendu Bhattacharyya, G.C.Layek, *Casson Fluid Flow over an Unsteady Stretching Surface,* Ain Shams Engineering Journal(2013), Vol. 4(4), pp. 933-938.

25. L. Roberts, *On the melting of a semi-infinite body of ice placed in a hot stream of air,* J. Fluid Mech.(1958), vol.4, pp.505-528.

26. T. Hayat, M. Farooq, and A. Alsaedi, *Melting heat transfer in the stagnation point flow of Maxwell fluid with doublediffusive convection,* Int. J. Numer. Methods Heat Fluid Flow(2014). vol.24, pp.760–774.

27. K. Das, *Radiation and melting effects on MHD boundary layer flow over a moving surface,* Ain Shams Eng. J.(2014), vol.5, pp.1207–1214.

28. E.M. Epstein, D.H. Cho, *Melting heat transfer in steady laminar flow over a flat plate*, J. Heat Transfer (1976), vol.98, pp.531-533.

29. M. Kazmierczak, D. Poulikakos, I. Pop, *Melting from a flat plate embedded in a porous medium in the presence of steady convection*, Numer. Heat Transfer (1986), vol.10, pp.571-581.

30. R.S.R.Gorla, M.A. Mansour, I.A. Hussanien, A.Y. Bakier, *Mixed convection effect on melting from a vertical plate*, Transport Porous Med.(1999) ,vol.36,pp.245-254.

31. N. Bachock, A. Ishak, I. Pop, *Melting heat transfer in boundary layer stagnation point flow towards a stretching/shrinking sheet*, Phys. Lett. A(2010), vol.374,pp.4075-4079.

32. A.J. Chamkha, A.M. Rashad, E. Al-Meshaiei, *Melting effect on unsteady hydrodynamic flow of a nanofluid past a stretching sheet,* Int. J. Chem. React. Eng. (2011), vol.9. Pp.1-13.

33. R.S.R. Gorla, A. Chamkha, A. Aloraier, *Melting heat transfer in a nanofluid flow past a permeable continuous moving surface,* J. Nav. Arch. Mar. Eng.(2011), vol.2, pp.83-92.

34. L.J. Grubka, K.M. Bobba, *Heat transfer characteristics of a continuous stretching surface with variable temperature*, ASME J. Heat Transf. (1985), vol.107, pp.248–250.

35. C.H. Chen, *Laminar mixed convection adjacent to vertical continuously stretching sheets*, Heat Mass Transf. (1998), vol.33, pp.471–476.

36. Rajesh Sharma, *Effect of viscous dissipation and heat source on unsteady boundary layer flow and heat transfer past a stretching surface embedded in a porous medium using element free Galerkin method*, Applied Mathematics and Computation (2012), vol.219(3), pp.976-987.

37. I.S. Oyelakin, S. Mondal, P. Sibanda, *Unsteady Casson nanofluid flow over a stretching sheet with thermal radiation, convective and slip boundary conditions,* Alex. Eng. J. 55 (2016) 1025–1035.

38. P. Mohan Krishna, N. Sandeep, J. V. Ramana Reddy and V. Sugunamma, *Dual solutions for unsteady flow of Powell Eyring fluid past an inclined stretching sheet,* Journal of Naval Architecture and Marine Engineering (2016), vol.13 (1), pp. 89-99.